Dynamic Source Effects of Dip-Slip Earthquake on Strong Ground Motion

DALGUER, Luis Angel and **IRIKURA**, Kojiro

Disaster Prevention Research Institute, Kyoto University, Uji Kyoto 611-0011, Japan

(e-mail: dalguer@egmdpri01.dpri.kyoto-u.ac.jp; irikura@egmdpri01.dpri.kyoto-u.ac.jp; phone: +81-774 38-4058, fax: +81-774-33-5866)

Abstract

The ground motion on dipping faults was observed that is larger in the hanging wall than in the footwall. In order to show that the ground motion is affected mainly by dynamic source effects, the rupture process of dipping faults with different asperity size but with the same seismic moment is modeled. The results suggest that the effect of the asperity size on ground motion is important in the generation of high frequency components. The smaller is the asperity, the more is the high frequency motion generation. Based on these results, we simulate the rupture process of the southern and northern part of the 1999 Chi-Chi (Taiwan) earthquake in order to explain the damage distribution on buildings caused by the earthquake in which, although the strongest ground motion occurred at the northern part of the causative fault, structural damage was heavier in the southern part than in the former.

Introduction

The recent 1999 Chi-Chi (Taiwan) earthquake (Ms= 7.6) had a serious impact in the international community of scientists and engineers devoted to seismology and earthquake engineering because of its complexity and uncommon characteristics. The earthquake originated on a low-angle reverse fault with a strike of nearly N5° E and a dip between 25° and 36° (Shin et al., 2000[1]). The rupture of the causative fault reached the surface and propagated along about 80km, starting at the southern and extending northwards of the Chelongpu fault, as shown in Figure 1a. Spectacular horizontal displacements up to 9.0 m and vertical offsets of 1.0m to 4.0m were registered along the surface rupture, being the largest on the northern zone. The damages caused by the earthquake show uncommon distribution. Although the largest displacements occurred at the northern part of the causative fault, structural damage was heavier in the southern part than in the former. Heavy damage happened mostly in the hanging wall side and less in the footwall side. Such differences in the damage distribution can be inferred from Figure 1b, which shows a comparison of the spectral pseudo-velocity from records of stations located at the northern (TCU052) and southern (TCU129 and TCU089) parts. The peak velocity for frequencies less than 1.0 Hz is larger in the northern part. On the contrary, for frequencies greater than 1.0 Hz, the peak velocity ground motion is larger in the southern part. It means that the northern part generated stronger ground motion in low frequency than the southern part. In order to get better understanding of the complex damage distribution caused by this earthquake, the rupture process was numerically simulated. Firstly we simulated the rupture process of three theoretical dipping faults with different size of asperity but with the same seismic moment. These simulations were made in order to study the effects of the asperity on the ground motion, the results show that the model with the smallest asperity generate stronger ground motion in high frequency.

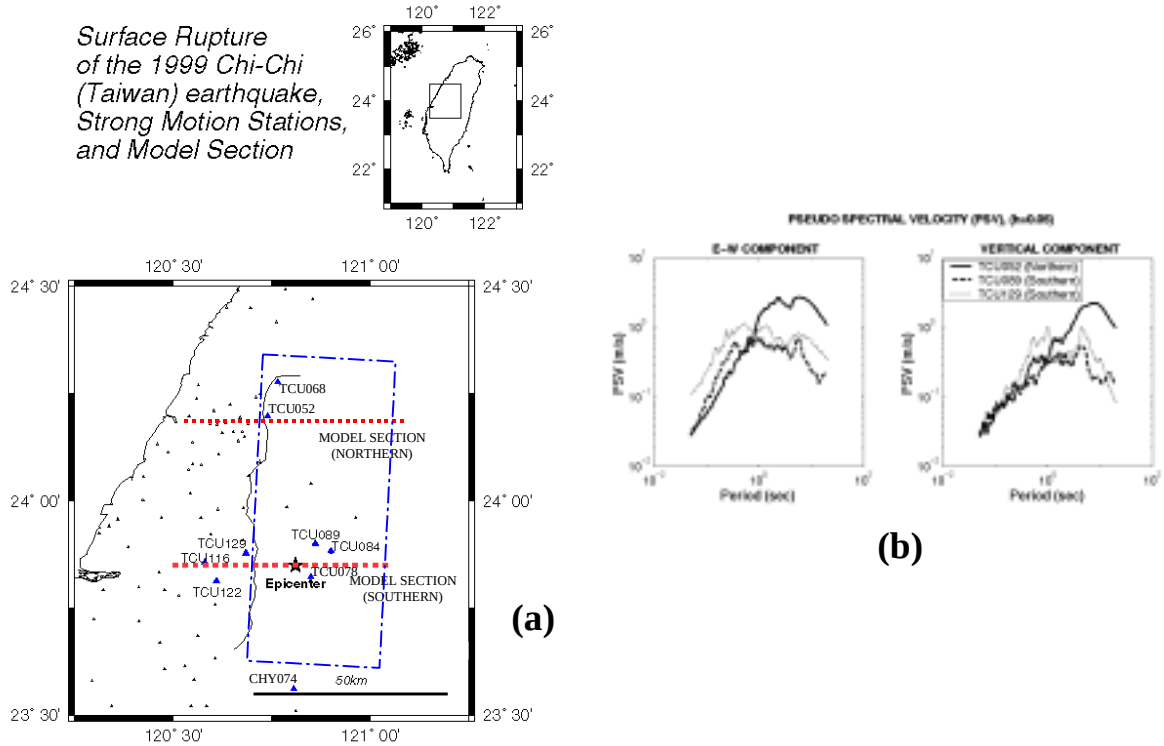

Figure1. a) Location of the surface rupture of the Chelongpu fault, stations records used for comparison, source model and sections of the northern and southern model; b) Comparison of pseudo spectral velocity for records of stations at the northern and southern parts.

Description of the numerical solution

The Discrete Element Method (DEM), used in the analysis, models any orthotropic elastic solid. It is constructed by a three dimensional periodic truss-like structure using cubic elements. Nayfeh and Hefzi, (1978[2]) established the equivalence requirements between the cubic arrangement and an orthotropic elastic medium. The method leads to results converging to solutions for a linear elastic continuum in dynamic problems. Riera and Rocha, (1991[3]) used an approach in fracture studies, Doz and Riera, (1995[4]) employed it to model the stick-and-slip motion along friction surfaces and Dalguer et al.,(1999[5]) evaluated the generation of foreshock and periodicity of earthquakes. In the discrete dynamic model, masses are concentrated at nodal points. The solids are represented as an array of normal and diagonal elements linking lumped nodal masses. The dynamic analysis is performed using explicit numerical integration in the time domain. At each step of integration a nodal equilibrium equation (Eq. 1) is solved by the central finite differences scheme.

$$m\ddot{u}_i + c\dot{u}_i = f_i \tag{1}$$

where m denotes the nodal mass, c the damping constant, u_i a component of the nodal coordinates vector and f_i a component of the resulting forces at one nodal point including elastic, external and frictional forces in direction i of the motion. In the current model, only the nodal points that coincide with the pre-existing fault, once it breaks, are subjected to frictional forces governed by the slip-weakening friction law. The damping constant c was assumed to be proportional to the rigidity (k) of the bars of every cubic element, that is $c=\xi k$, where ξ was assumed to be 0.005.

Simulation of dipping faults with different asperity size

Figure 2a shows the fault model used to simulate the rupture process of a dipping fault, the simulation is made for different asperity size but with the same seismic moment:
Model 1: Length of asperity L =6km, Stress drop on the asperity $\Delta\sigma$=9.0Mpa.
Model 2: Length of asperity L =8km, Stress drop on the asperity $\Delta\sigma$=5.0Mpa.
Model 3: Length of asperity L =10km, Stress drop on the asperity $\Delta\sigma$=3.2Mpa
All the models share the following common assumptions:
-There is a surface sedimentary layer with a depth of 4km characterized by a set of P wave velocity (4.3 km/sec), S wave velocity (2.5 Km/sec), density 2500 kg/m^3. The basement (seismogenic zone) is a homogeneous medium with P wave velocity (6.1 km/sec), S wave velocity (3.5 Km/sec), density 2700 kg/m^3.
-The slip-weakening friction model is adopted as the constitutive relation for the fault.
-The stress drop along the fault plane in the shallow surface layer is negligible.
-The ultimate stress, i.e. the strength excess on the fault surface in the shallow surface layer increases linearly with depth and, in order to avoid any fault opening, we applied a normal stress along the fault, equivalent to the strength excess.
-The critical slip (*Dc*) along the fault is larger near the surface than at greater depths.
The main results of these simulations are shown in Figure 2b. The final displacements along the free surface are almost the same for the three models, it is because all the models has the same seismic moment. But if we observe the peak velocity along the fault, the model with asperity length L=6km shows higher values than the others. This difference increase when the ground motion is filtered in a frequency range of 0.5Hz to 2.0Hz. These results suggest that the higher frequency motion could be generated by the model with smallest size of asperity.

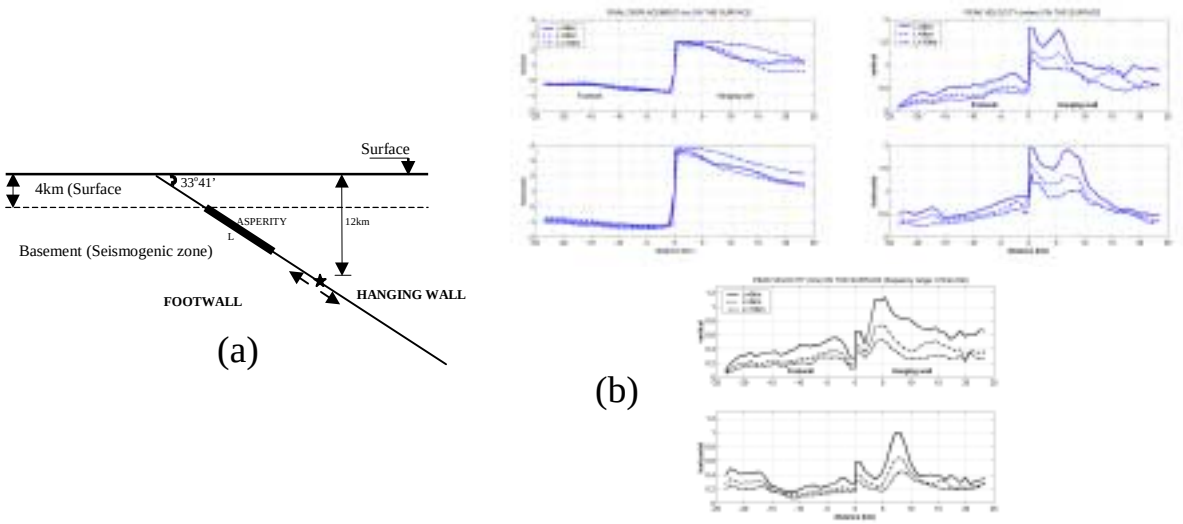

Figure 2. a) Fault model used for the dynamic simulation of dipping faults with different asperity size (L=6km, L=8km and L=10km); b) Comparison of the final displacement and peak velocity on the surface between the three models with different size asperity.

Dynamic rupture process simulation of the 1999 Chi-Chi (Taiwan) earthquake

Since the faulting process appears to have been nearly pure thrust along the various fault segments, a 2D model was employed to perform a dynamic simulation of the rupture process of the fault and the near-fault ground motion. On account of the differences in the observed features of the rupture process in the northern and southern parts of the causative fault of the 1999 Chi-Chi (Taiwan) earthquake, each part was modeled independently. The location of the two models sections along the surface rupture is shown in Figure 1a. The first model (southern part) is near the epicentral area and the second model (northern part) is near the TCU052 station. The parameters used for the dynamic simulation and the geometry of the two fault models are shown in Figure 3. Both models share the same common assumptions used for the three theoretical models shown in the last item. In the model for the southern part the existence of only one asperities with small width (6 km) and stress drop of 3Mpa were admitted in the basement underlying the sediments. The northern part, on the other hand, is assumed to have an asperity with larger width (15km) and higher stress-drop (between 1.5 MPa and 8MPa).The main results of the simulation are as follow: the comparison of the ground motion on the surface between the northern and southern model (in a frequency range up to 2.00 Hz) is shown in Figure 4. This Figure shows the final displacements, peak velocity and peak velocity in a frequency range of 0.5 to 2.0Hz. From Figures 4a and 4b we find that the final displacement and the peak velocity are larger in the northern model than in the southern model. However, when the ground motion velocities are filtered in a frequency range of 0.5 to 2.0Hz as shown in Figure 4c, the peak velocities are larger in the southern model than in the northern model. These results suggest that the northern model predicts stronger ground motion than the southern model in lower frequency, however, in higher frequency between 0.5 to 2.0 Hz (natural frequency range of standard structures) the ground motion is stronger in the southern model. From these results we can conclude that even the northern model shows stronger ground motion, the most severe damages in structures could happen in the southern model because the southern model has more possibilities to excite severely the fundamental frequency of standard structures.

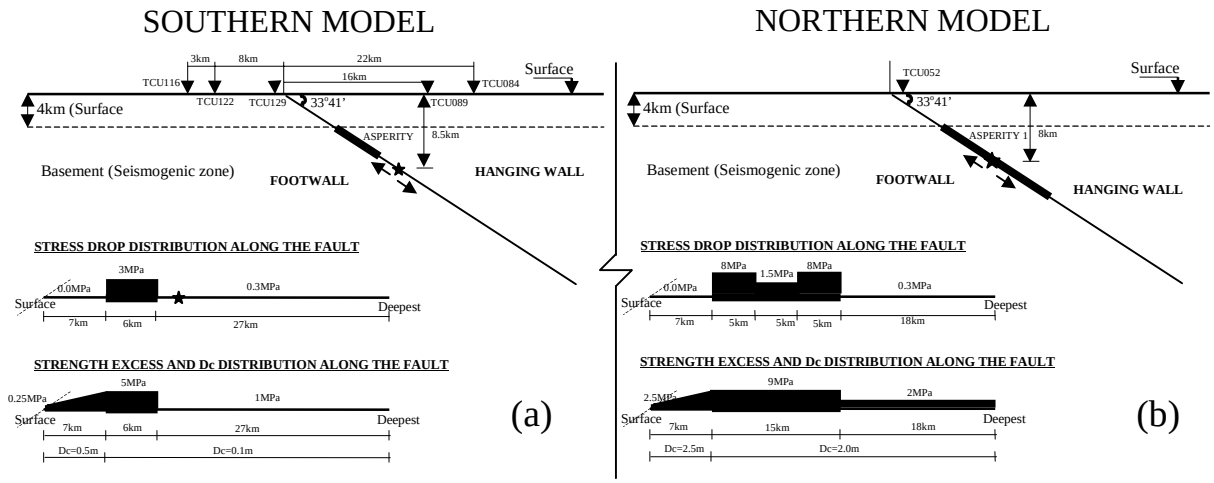

Figure 3. Fault models and parameters distribution used for the dynamic simulation: (a) southern model, (b) northern model.

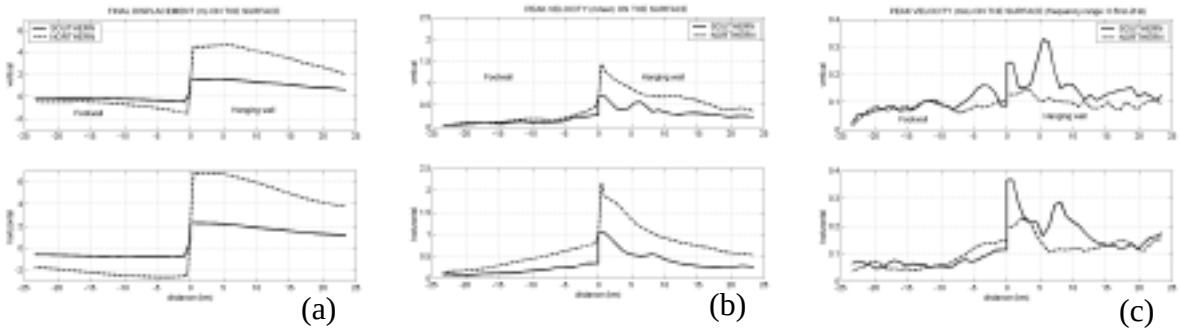

Figure 4. Comparison of the final displacement and peak velocity on the surface between the northern model and southern model: (a) Final displacement, (b) peak velocity (c) peak velocity in a frequency range of 0.5 to 2.0 Hz.

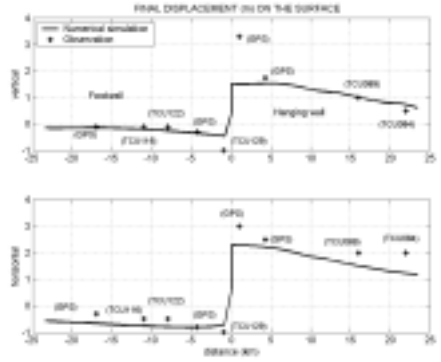

Figure 5. Comparison between the numerical simulation and the observations (GPS data and stations records) of the final displacements along the surface near the epicentral area (southern model).

In order to validate the dynamic model studied here, we compared our results with the observations. Figure 5 shows that the southern model predicts final vertical displacement of about 2.0m and horizontal displacement of about 3.3m in the hanging wall that agree satisfactorily with those obtained by the GPS data and the final displacements of the station records. In Figure 6a to 6e we also compare the waveform of the displacement and velocity ground motions of east-west and vertical components recorded at five stations near the surface rupture of the epicentral area (stations TCU084, TCU089 on the hanging wall side and TCU129, TCU116 and TCU122 on the footwall side). We find that the main characteristics of the recorded ground motion are adequately reproduced, as observed in the simulated and observed time-histories. In the frequency range from 0.5Hz to 1.0Hz, although obtained with a 2D model, the ground motion simulation qualitatively matches the observations. And also for the northern model we succeed in doing the simulation of the ground motion recorded of TCU052 station as shown in Figure 6f in which the comparison of the simulation fit very well with recorded. The dynamic models presented in this paper showed that the effects of the dynamic source mechanism on strong ground motion are fundamentally important in the ground motion prediction and the assessment of seismic hazard.

Acknowledgments

We thank the Seismology Center, Central Weather Bureau (CWB), Taipei, Taiwan for providing the Digital waveform files corresponding to the accelerograms of the stations used.

References

[1] Shin T. C., Kuo, K.W., Lee, W.H.K, Teng, T.L. and Tsai, Y.B, 2000, *A preliminary report of the 1999 Chi-Chi (Taiwan) earthquake*, Seism. Res. Lett., **71**, 24-30.

[2] Nayfeh, A.H. and Hefsy, M.S., 1978, *Continuum modeling of three-dimensional truss-like space structures*, AIAA Journal, **16**, 779-787.

[3] Riera, J.D. and Rocha, M.,1991 *A note on the velocity of crack propagation in tensile fracture*, Revista Brasileira de Ciencias Mecanicas, RBCM, **XII, N3**, 217-240.

[4] Doz G.N and Riera J.D., 1995, *Towards the numerical simulation of seismic excitation trans-action*, 13th International Conference on Structural Mechanics in Reactor Technology (SMiRT13), Porto Alegre, Brazil, **3**.

[5] Dalguer. L.A., Riera J.D and Irikura, K., 1999, *Simulation of seismic excitation using a stick-slip source mechanism*. Transaction, 15th International Conference on Structural Mechanics in Reactor Technology (SMiRT15), Seoul, Korea, **7**, 13-18.

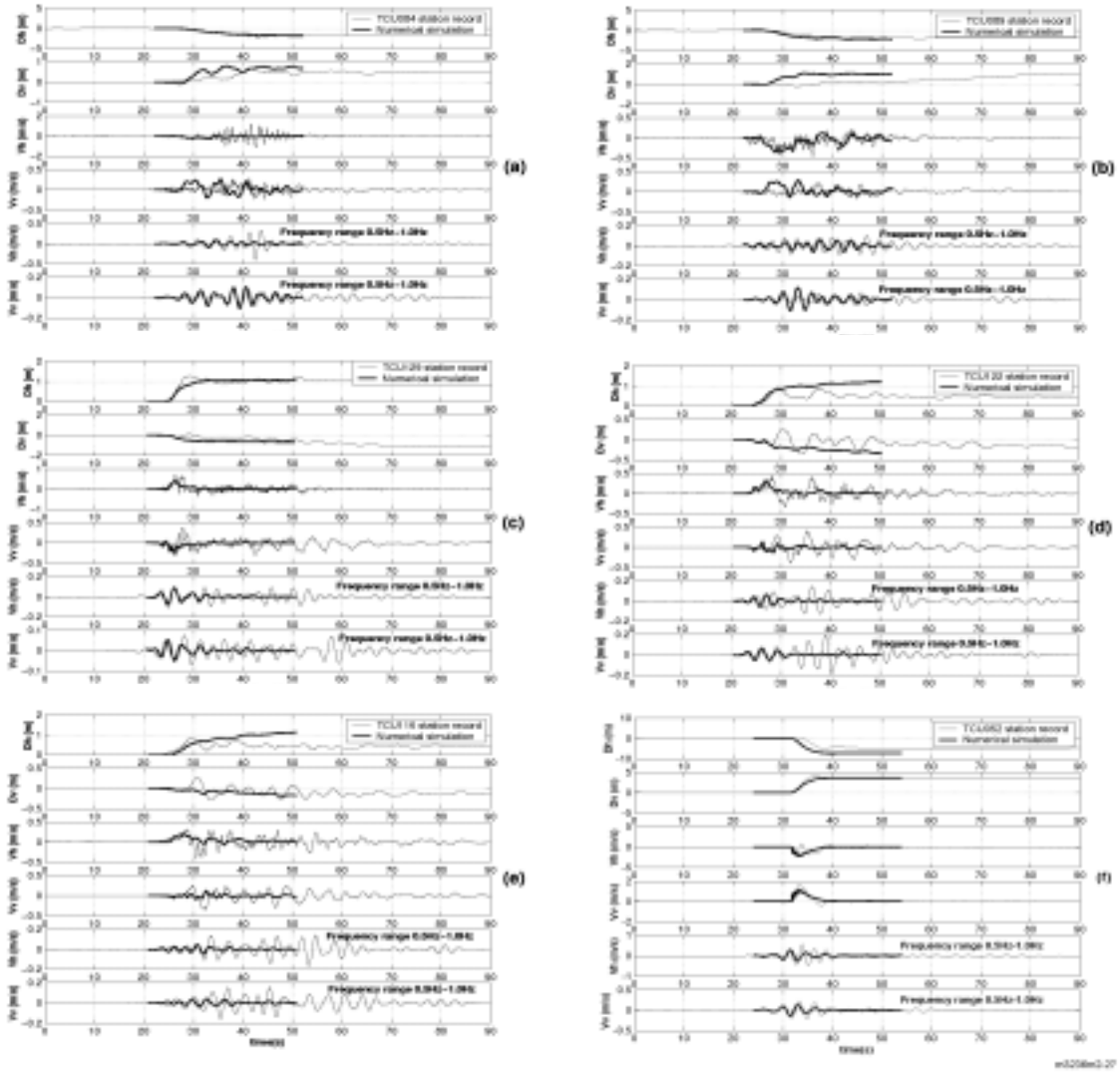

Figure 6. Comparison of the numerical simulation with stations records of horizontal (E-W) and vertical component of displacement, velocity and velocity in frequency range of 0.5Hz to 1.0Hz: (a) for TCU084 station, (b) for TCU089 station, (c) for TCU129 station, (d) for TCU122 station, (e) for TCU116 station, (f) TCU052 station. *Dh* and *Dv* are the horizontal (east-west) and vertical component respectively and *Vh* and *Vv* are the horizontal (east-west) and vertical component of velocity ground motion respectively